AD-A130 790 THE EFFECTS OF POWDER METALLURGICAL PROCESSING AND INTERMEDIATE THERMAL M..(U) GEORGIA INST OF TECH ATLANTA FRACTURE AND FATIGUE RESEARCH LA.. 1/1

UNCLASSIFIED V KUO ET AL. 1983 ARO-17161.6-MS F/G 11/6 NL

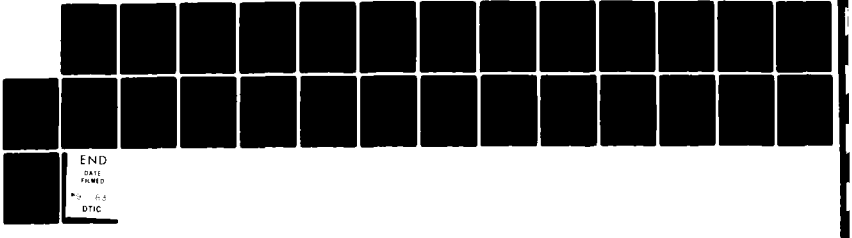

END
DATE FILMED
DTIC

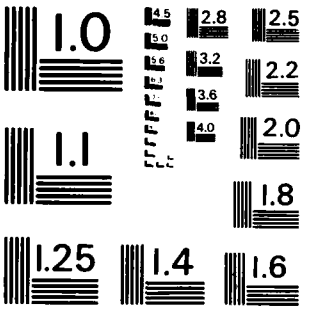

MICROCOPY RESOLUTION TEST CHART
NATIONAL BUREAU OF STANDARDS - 1963 - A

Unclassified
SECURITY CLASSIFICATION OF THIS PAGE (When Data Entered)

ARO 17161.6-MS

REPORT DOCUMENTATION PAGE

READ INSTRUCTIONS BEFORE COMPLETING FORM

1. REPORT NUMBER
2. GOVT ACCESSION NO. AD-A130790
3. RECIPIENT'S CATALOG NUMBER

TITLE (and Subtitle)
The Effects of Powder Metallurgical Processing and Intermediate Thermal Mechanical Treatment on the Fatigue Properties of High Strength Aluminum Alloys

5. TYPE OF REPORT & PERIOD COVERED
Final Report
1 April 1980 - 31 March 1983

6. PERFORMING ORG. REPORT NUMBER

AUTHOR(s)
Victor Kuo, H. Chang, and E.A. Starke, Jr.

8. CONTRACT OR GRANT NUMBER(s)
DAAG29-80-C-100

PERFORMING ORGANIZATION NAME AND ADDRESS
Fracture and Fatigue Research Laboratory

10. PROGRAM ELEMENT, PROJECT, TASK AREA & WORK UNIT NUMBERS

CONTROLLING OFFICE NAME AND ADDRESS
U. S. Army Research Office
Post Office Box 12211
Research Triangle Park, NC 27709

12. REPORT DATE

13. NUMBER OF PAGES
21

MONITORING AGENCY NAME & ADDRESS (if different from Controlling Office)

15. SECURITY CLASS. (of this report)
Unclassified

15a. DECLASSIFICATION/DOWNGRADING SCHEDULE

16. DISTRIBUTION STATEMENT (of this Report)

Approved for public release; distribution unlimited.

17. DISTRIBUTION STATEMENT (of the abstract entered in Block 20, if different from Report)

JUL 2 8 1983

A

18. SUPPLEMENTARY NOTES

The view, opinions, and/or findings contained in this report are those of the author(s) and should not be construed as an official Department of the Army position, policy, or decision, unless so designated by other documentation

19. KEY WORDS (Continue on reverse side if necessary and identify by block number)

powder metallurgy, aluminum alloys, fatigue, rapid solidification, thermomechanical processing

20. ABSTRACT (Continue on reverse side if necessary and identify by block number)

The application of advanced metallurgical processing techniques, e.g., intermediate thermomechanical treatment (ITMT) and powder metallurgy (P/M), has produced a recrystallized X7091 P/M alloy having fine grain and particle structures and weak texture with the best overall mechanical properties compared to those of ingot metallurgical and conventional P/M alloys. The dependence of mechanical properties on grain size and particle distribution has been demonstrated among these alloys. The

DD FORM 1 JAN 73 1473 EDITION OF 1 NOV 65 IS OBSOLETE

UNCLASSIFIED
SECURITY CLASSIFICATION OF THIS PAGE (When Data Entered)

20. continued

study of the effect of the last microstructural feature, crystallographic texture, is necessary for further property improvement through texture control.

A sharp retained deformation texture and a weak texture were introduced into two recrystallized P/M plates with similar grain size (about 15 μm) and fine particle distribution by ITMT's based on different recrystallization mechanisms. The difference in strength was mainly accounted for by the different values of Taylor factor with respect to the stress axis. Although the tensile fracture properties were similar, the fracture appearance varied with the degree of grain boundary misorientation. The texture effect on the stress-controlled fatigue appeared to be the modification in strength, even though the crack initiation mechanisms were different. The change in initiation mechanism was associated with the change in grain boundary misorientation and slip length. The variation in texture changed the crack morphology, deformation behavior and slip length during fatigue crack propagation. These factors led to a different degree of roughness-induced crack closure and slip reversibility at the crack tip, and resulted in the difference in crack growth rate. The improvements in strength and fatigue resistances have been obtained simply by introducing a sharp retained deformation texture into a recrystallized X7091 P/M plate.

The Effects of Powder Metallurgical Processing and Intermediate Thermal Mechanical Treatment on the Fatigue Properties of High Strength Aluminum Alloys

Final Report on Grant No.
DAAG29-80-C-100
April, 1983

by

Victor Kuo, H. Chang and E. A. Starke, Jr.
Fracture and Fatigue Research Laboratory
Georgia Institute of Technology
Atlanta, GA 30332

This Research was sponsored by the Army Research Office,
Research Triangle Park, NC under Grant Number DAAG29-80-C-100

TABLE OF CONTENTS

LIST OF FIGURES

ABSTRACT

The application of advanced metallurgical processing techniques, e.g., intermediate thermomechanical treatment (ITMT) and powder metallurgy (P/M), has produced a recrystallized X7091 P/M alloy having fine grain and particle structures and weak texture with the best overall mechanical properties compared to those of ingot metallurgical and conventional P/M alloys. The dependence of mechanical properties on grain size and particle distribution has been demonstrated among these alloys. The study of the effect of the last microstructural feature, crystallographic texture, is necessary for further property improvement through texture control.

A sharp retained deformation texture and a weak texture were introduced into two recrystallized P/M plates with similar grain size (about 15 μm) and fine particle distribution by ITMT's based on different recrystallization mechanisms. The difference in strength was mainly accounted for by the different values of Taylor factor with respect to the stress axis. Although the tensile fracture properties were similar, the fracture appearance varied with the degree of grain boundary misorientation. The texture effect on the stress-controlled fatigue appeared to be the modification in strength, even though the crack initiation mechanisms were different. The change in initiation mechanism was associated with the change in grain boundary misorientation and slip length. The variation in texture changed the crack morphology, deformation behavior and slip length during fatigue crack propagation. These factors led to a different degree of roughness-induced crack closure and slip reversibility at the crack tip, and resulted in the difference in crack growth rate. The improvements in strength and fatigue resistances have been obtained simply by introducing a sharp retained deformation texture into a recrystallized X7091 P/M plate.

Introduction

Current studies[1-9] of high-strength Al-Zn-Mg-Cu (7XXX) alloys have focused on the development of powder metallurgical (P/M) alloys. The P/M X7091 alloy has shown improved monotonic, fatigue strength and resistance to stress corrosion cracking but inferior fracture toughness and resistance to fatigue crack propagation (FCP) when compared with ingot metallurgy (I/M) alloys.[1-4] Our initial studies involved microstructural modifications of X7091 using a variety of processing methods in order to obtain a better combination of mechanical properties.[1] With the exception of one product which had oxide-induced fracture, a reduction in grain size and a finer particle distribution increased the ductility and resistance to fatigue crack initiation (FCI) but decreased the resistance to FCP. An optimum microstructure, which consisted of small recrystallized grains, a fine particle distribution and a weak texture, was identified as having the best overall mechanical properties among the various microstructures studied. The details of this work were published recently in Metallurgical Transactions (Ref. 1), which is attached as Appendix A. In addition, we have conducted further studies on I/M X7091. That work is covered in the M.S. Thesis of H. Chang which is attached as Appendix B. Our most recent work, which will be covered in this final report, is directed towards further improvement in properties through texture control.

The non-uniform material flow during metal working and/or variations in heat-up rate during subsequent heat treatment usually result in differences in grain structure and texture throughout the thickness of most

high-strength aluminum products. Since particles greatly affect the recrystallization process, the presence of a uniform particle distribution may reduce the inhomogeneity of a recrystallized microstructure. In general, widely-spaced, coarse particles create strain concentrations at particle-matrix interfaces, while closely-spaced fine particles tend to lead to more uniform dislocation distribution after metal working. During subsequent annealing, the acceleration of recrystallization is usually associated with the former case, while retardation is associated with the latter case. The intermediate thermomechanical treatment (ITMT) of aluminum alloys is a practice of the former case. For a certain amount of reduction, the recrystallized grain size is closely related to the number density of coarse particles. The resulting texture depends on the predominant recrystallization mechanism.

The effect of texture on the strength of materials as predicted by the Taylor relationship has been generally accepted. Palmer et al[10] reported that the yield strength of an Al-Li P/M alloy decreased with the sharpness of the fiber texture, which decreased with increasing extrusion aspect ratio. This can be explained by the fact that most of the slip systems in the round-bar extrusion were unfavorably oriented for slip with respect to the tensile axis. When a material having planar slip characteristics, a fine particle distribution, and a random or weak texture is deformed, the grain boundaries can act as effective barriers to dislocation slip due to the high degree of grain boundary misorientation. The generation of multiple slip near grain boundaries to accommodate their incompatibility may result in more homogeneous deformation. The effectiveness of the grain boundary as a slip barrier decreases when the alignment of slip planes occurs in adjacent grains

of a sharply-textured material. In this case, the slip length is no longer limited to grain dimensions. The combined effects of the crystallographic orientation (with respect to stress axis) and slip length on deformation and fracture behavior may conclude the effect of texture on mechanical properties of a material.

Based on recrystallization theories and ITMT techniques, two annealing textures or texture intensities were introduced into a recrystallized P/M X7091 plate, while keeping other microstructural variables constant. Their effect on the monotonic and cyclic properties of this alloy will be described in this report.

Experimental

An extruded P/M X7091-T7E70 rectangular bar, having an unrecrystallized grain structure and a sharp extrusion texture, was commercially purchased from Alcoa, Alcoa Center, Pennsylvania. It was subjected to two ITMT's (Fig. 1) to produce two plates with similar recrystallized grain and particle structures but different textures. The Graff-Sargent etching solution was used to reveal the grain structure. Bromine etching was used to observe the particle distribution. Both plates showed fairly homogeneous grain and particle distributions throughout the thickness.

Crystallographic texture determinations were carried out using the x-ray reflection method. Fixed time increments were employed to collect intensity data over a polar orientation range from 0 to 70 degrees. A computer program was used to construct the pole figures in the form of equal value contours and to provide average, maximum and minimum

intensities. The higher-temperature rolled plate, designated as S, showed a higher degree of texture variation throughout the thickness than that of the lower-temperature rolled plate, designated as W.

In order to assess the effect of texture on the mechanical properties of an age-hardening alloy, it is convenient to choose an aging condition for which the effect of crystallographic orientation and grain boundary misorientation on deformation and fracture characteristics are most pronounced. In the peak-aged temper, dislocations shear the coherent and partially-coherent strengthening precipitates. Consequently, the deformation mode is predominantly planar and the effectiveness of the grain boundary as the slip barrier can be detected. Both plates were stretched 2.0 pct after being cold-water quenched from the recrystallization temperature and then aged to produce the peak strength, designated as T651.

All mechanical tests were performed on a closed loop servohydraulic machine. The flat specimens of 2.5 mm thick were selected from the thickness which possessed the highest contrast in texture between these two plates, with the stress axes parallel to the rolling direction. The specimens had a gauge width of 6.4 mm and a gauge length of 25.4 mm for the tensile tests. The tension-tension (R = 0.1), stress-controlled, high cycle fatigue (HCF) tests were conducted in a vacuum environment ($<2 \times 10^{-5}$ torr), with a frequency of 20 Hz, using specimens of 60 mm X 10 mm with a semi-round side notch (radius = 3 mm). Crack propagation tests were conducted in a vacuum environment, with R ratio of 0.1 and frequency of 30 Hz. The WOL-type, compact-tension specimens (H/W = 0.97) were used, and the crack propagated on a plane normal to the rolling

direction. A clip-on gauge was mounted at the end of the notch to measure the crack opening displacement periodically. A travelling microscope was equipped to measure the crack length, a, for every 0.3 mm after the crack advanced out of the plastic zone of previous loading within the ranges of plane strain condition and a/w's = 0.3-0.5. SEM was used to examine the fracture features.

RESULT AND DISCUSSION

Texture and Microstructure

The ITMT's used produced two differently textured, recrystallized plates with similar grain and particle structures. The pole figures from (111) reflections were utilized to interpret the textures tnrough the plate thickness, and the x-ray diffracted intensities were also normalized with the aid of a randomly oriented powder sample. The texture varied from {110} <112> near the surface to a sharp {110}<001> at the center of the S plate. Actually, the {110}<001>is a compromise texture of {110}<112>, and the latter has been recognized as a retained deformation texture. The ratio of maximum intensity to average intensity ranged from 6 to 13 in this plate. The W plate had texture varying from a weak cube near the surface to a weak {110}<112> at tne center, and the intensity ratio ranged from 2 to 4. Cube texture is a normal recrystallization texture for fcc materials. The difference in texture between these two plates may be associated with the difference in rolling temperatures, which produced different recrystallization mechanisms. The strain concentrations in deformation zones around the overaged particles after rolling

promoted particle-stimulated recrystallization during subsequent annealing, for the lower-temperature rolled W plate. The resulting weak texture was expected in accordance with the annealing texture formation theory developed by Humphreys[11] for a polycrystalline dispersion material. Dynamic recovery becomes more important with increasing rolling temperatures, therefore, the higher-temperature rolling produced a more homogeneously, deformed structure, which promoted continuous recrystallization and strain-induced grain boundary migration. This resulted in a sharp retained deformation texture for the S plate. The variation of texture through the thickness was mainly due to the non-uniform strain distribution during rolling and variations in heat-up rate during annealing from the surface to the center. Even though the variation was present, a very distinct texture difference existed between these two plates since they recrystallized by different mechanisms.

The samples for testing were selected from the center portion of the S plate with the intensity ratios ranging from 9 to 13, and from the portion slightly off the center of the W plate with the intensity ratio ranging from 2 to 4. The grain structure within these thicknesses had a grain diameter of a sphere with equivalent volume of about 15 μm and a grain shape parameter of about 0.32. Bromine etching showed a random distribution of particles with sizes less than 1 μm, which was similar to the particle structure of the as-received material. Therefore, most of the overaged coarse precipitates formed during extensive overaging were re-dissolved during the final anneal of the ITMT's. The heat treatments did not alter the fine distribution of dispersoids and constituent particles of the P/M alloy. Oxide stringers and clusters

had been broken up, although oxides were occasionally observed at the recrystallized grain boundaries during TEM studies. These two types of samples had similar grain and particle structures, but differed in the recrystallization texture by a factor of about 4.

Monotonic Properties

The monotonic properties obtained from the tensile testings are presented in TABLE I. The S plate showed an increase in yield strength (30 MPa) and elongation but a slightly lower value of reduction in area or ductility, compared to those of the W plate.

TABLE I. The monotonic properties of the differently-textured recrystallized plates at the T651 condition.

	Y.S. (MPa)	UTS (MPa)	Elongation (%)	$\ln\frac{A_o}{A}$ (%)
S plate	558	587	12.9	29
W plate	528	571	10.8	33

Y.S. = proof stress, $\sigma_{0.2}$

$\ln\frac{A_o}{A}$ = ductility from reduction in area

The strengtn of an age hardening aluminum alloy is primarily associated with precipitation strengthening although texture strengthening and grain boundary strengthening may also contribute. Since the aging condition and grain structure were similar in both plates, the difference in yield strength should be attributed to the difference in crystallographic orientation. According to the restricted slip theory for axisymmetric deformation, slip in the S plate had a lower-bound Taylor factor

value of about 2.45 compared to 2.24 for a randomly oriented polycrystalline material. This predicts a slightly higher strength for the S plate. The ratio of UTS/YS may indicate the degree of strain hardening during uniform deformation. The generation of more slip systems (multiple slip or homogeneous slip), due to the crystallographic orientation or to the grain boundary incompatibility, may be responsible for the higher degree of strain hardening of the W plate. The texture effect on strength and deformation may be associated with the crystallographic orientation dependence of slip activation and the promotion of homogeneous slip due to grain boundary misfit.

Both plates showed a shear-type, transgranular fracture. Fracture occurred by microvoid coalescence and the fracture surface of the S plate consisted of a relatively shallow dimple structure, while the secondary cracking along grain boundaries was an important fracture feature for the W plate. The uniform deformation throughout the gauge length yielded a slightly higher elongation of the S plate due to the similar orientation of the most grains. The shallow dimple structure may indicate that one slip system predominated up to fracture, consistent with the observed crystallographic texture. In contrast, the non-uniform distribution of strain may lead to early void nucleation at the grains which are favorably oriented for slip. This resulted in a slightly lower elongation and higher reduction in area for the W plate. However, the secondary cracking along these highly misoriented grain boundaries did not contribute a pronounced effect to the fracture properties of this plate.

The variation in recrystallization texture resulted in different

strength and other tensile properties. The effect of slip length was obscured, since the S plate did not show the characteristics of larger grains, e.g. low yield strength and low ductility.

Fatigue Crack Initiation

The S-N plots of the HCF tests are shown in Fig. 2a. There was a very slight degree of experimental scatter, compared to that of the other I/M 7XXX alloys, due to the homogeneous microstructures of these P/M alloys. The S plate showed a better FCI resistance in the long-life region. The FCI sites were located at the center of the specimen thickness. The cracks initiated at the slip bands, which covered several grains in the S plate, but were at both slip bands and grain boundaries in the W plate.

The strength of a material is usually the most significant factor in stress-controlled HCF. Fig. 2b illustrates the S-N curves normalized with the yield stresses in TABLE I. They became coincident with the modification of strength. Therefore, the texture effect on stress-controlled HCF was mainly due to its effect on the strength of these plates. However, the FCI mechanisms were different. The slip band initiation, which extended across about 4-8 grains, may have indicated that the slip distance may be several times the grain dimension of the S plate. Furthermore, this phenomenon may have been enhanced by the formation of persistent slip bands or strain localization which increased the stress concentration level at the intersection with the slightly-misoriented grain boundaries. Consequently, the resistance to FCI may be degraded since fatigue life normally decreases with increasing grain

size or slip length. On the other hand, the highly-misoriented grain boundaries promoted homogeneous deformation, which reduced the degree of strain localization, and eliminated the slip band cracking as the initiation mechanism. Such an improvement in FCI resistance has been reported for several aluminum alloys.[12,13] In the short-life region in Fig. 2b, the fatigue lives followed the trend described above. The difference became obscured with increasing fatigue life. This may be due to a very small amount of plastic strain being generated at the low stress amplitudes. Although the mechanisms for crack initiation were different, the effect of texture on the HCF lives was mainly accounted for by the difference in strength. Introduction of a weak texture may have improved the FCI resistance in the short-life region, but a sharp texture may have improved the resistance in the long-life region.

Fatigue Crack Propagation

Two sets of fatigue crack growth rate (FCGR) data were generated from a/w = 0.3 to 0.4 and 0.4 to 0.5, respectively. The stress intensity factor range (ΔK) was limited below 10 MPa $\sqrt{m}$ for the plane strain condition in this type of thin compact-tension specimen to be valid. Fig. 3 presents the FCGR's as a function of ΔK for the S and W plates. The FCGR's collected from a/w = 0.3 to 0.4 were about one order greater than those from a/w = 0.4 to 0.5. The crack in the S plate advanced slower than that in the W plate for the same a/w value range. The crack propagation was mostly transgranular and grew in a zig-zag fashion. The fracture features consisted of brittle facets at various angles with respect to the stress axis. The average facet size of the S fracture surface was several times that of the grain size, while the W fracture

surface had a facet size roughly corresponding to the grain size. The difference in FCGR's may be attributed to the difference in strength, deformation behavior, slip length and/or the degree of roughness-induced crack closure between these two differently-textured plates.

The accumulated damage model indicates that the crack advances when a maximum amount of plastic deformation has been accumulated at the crack tip. The strength of a material usually has less influence on the FCGR, compared to its cyclic ductility and cyclic strain hardening exponent. Fatigue crack closure may also have an effect on the FCGR. The crack closure stress intensity factor, K_c, derived from the crack opening displacement, was plotted against the FCGR's of these two plates in Fig. 4 for different a/w values. The K_c's were larger for propagation over a/w values between 0.4 and 0.5 than for a/w values between 0.3 and 0.4. The longer crack appears to have experienced a higher degree of crack closure. There was significant scatter in the K_c data as shown in Fig. 4. However, the S cracks showed slightly larger values of K_c than those of the W cracks. Since most of the grains had a similar crystallographic orientation, the crack front did not change propagation direction dramatically as it crossed the grain boundaries, until other crack planes became preferred mechanically. This phenomenon yielded a fracture surface with large facets, which had experienced a higher degree of roughness-induced crack closure compared to the fine-faceted W fracture surface. Consequently, the rougher fracture surface slowed down the fatigue crack growth in the sharply-textured S plate.

In order to understand the effects of deformation behavior and slip length on FCGR's of these two plates, ΔK_{eff}, substrating K_c from

K_{max}, is used to represent the ΔK at which the crack actually propagated. Figure 5 shows the FCGR's as a function of ΔK_{eff}. The S plate has slower FCGR's than those of the W plate, despite the wide scatter bands due to the scattered K_c values. According to the accumulated damage model, the less the plastic deformation is accumulated at the crack tip, the slower the fatigue crack grows. With the consideration of crystallographic texture, under a certain amount of normal stress, the plastic strain response of the S plate was smaller due to its larger Taylor factor value with respect to the stress axis. Since the grain boundary did not act as an effective barrier to dislocation slip in a sharply-textured material, the slip length was probably larger than the grain dimension of the S plate. The large facets on the fracture surface were partially a result of this phenomenon. The studies of grain size dependence of FCGR have indicated that the dislocation slip was more reversible on a long slip band during fatigue.[14] Therefore, the less plastic strain response and the more reversible slip reduced the accumulation rate of plastic deformation at the crack tip for the S plate. In contrast, a higher accumulation rate may have occurred in the W plate, because of its homogeneous deformation, generation of geometrically-necessary dislocations at grain boundaries and less reversible slip on a short slip band. Consequently, the different deformation behavior resulted in the difference in FCGR's between S and W plates.

The effect of recrystallization texture on the FCGR's in these two materials, included its effect on crack morphology, slip length and deformation behavior. The amount of plastic strain response during each loading cycle was determined by the crystallographic orientation.

The increase in texture sharpness increased the fracture surface roughness and slip length, but reduced the slip homogeneity. Roughness-induced crack closure and the accumulated damage model suggest that all these factors reduced the FCGR of the sharply-textured S plate. Further improvement on the resistance to FCP of the 7XXX alloys may be accomplished by introducing a sharp retained deformation texture in a recrystallized P/M alloy.

CONCLUSIONS

1. Two recrystallized plates having similar grain and particle structures, but different textures (or texture intensities) by a factor of 4, were produced by ITMT's based on different recrystallization mechanisms.
2. The variation in strength was related to the difference in the Taylor factor value with respect to the stress axis. The sharply-textured plate showed a greater yield strength (about 30 MPa).
3. The tensile fracture appearance varied with the degree of grain boundary misorientation. Although the two plates had similar fracture properties, secondary cracking along grain boundaries was prevalent in the weakly-textured plate.
4. The texture effect on the stress-controlled HCF appeared to be the modification in strength, although the FCI mechanism may also change. The cracks were initiated at slip bands, which covered several grains in the sharply-textured plate, and at both slip bands and grain boundaries in the weakly-textured plate. The change

in FCI mechanism was associated with the change in grain boundary misorientation and slip length.

5. The variation in texture changed the crack morphology, deformation behavior and slip length during FCP. The coarse fracture features enhanced the roughness-induced crack closure. Also, a longer slip distance and greater slip reversibility reduced the accumulation rate of plastic strain at the crack tip. All these factors led to the higher FCP resistance of the sharply-textured plate.
6. The further improvement in overall mechanical properties, which included a higher strength, longer HCF lives and greater FCP resistance, was obtained by introducing a sharp retained deformation texture into a recrystallized X7091 P/M plate.

SCIENTIFIC PERSONNEL

Dr. Edgar A. Starke, Jr., Co-Principal Investigator

Dr. Saghana B. Chakrabortty, Co-Principal Investigator

Victor W.C. Kuo, Graduate Student
M.S. Georgia Institute of Technology
PhD Georgia Institute of Technology expected August, 1983

Hao Chang, Graduate Student
M.S. Georgia Institute of Technology, June, 1983

Publications and Technical Reports

1. Victor W.C. Kuo and E.A. Starke, Jr., "The Effects of ITMT's and P/M Processing on the Microstructure and Mechanical Properties of the X7091 Alloy" in Michael J. Koczak and Gregory J. Hildeman, eds., High Strength Powder Metallurgy Aluminum Alloys, The Metallurgical Society of AIME, Warrendale, PA, 1982 pp. 41-63.

2. Victor W.C. Kuo and E.A. Starke, Jr., "The Effect of ITMT's and P/M Processing on the Microstructure and Mechanical Properties of the X7091 Alloy," Met. Trans. A. 14A (1983) pp. 435-447.

3. Hao Chang, "The Effect of an Intermediate Thermomechanical Treatment on the Fatigue Properties of I/M X7091 Aluminum Alloy," M.S. Thesis, Georgia Institute of Technology, Atlanta, GA, June, 1983.

4. Victor W.C. Kuo, "The Effects of Powder Metallurgical Processing and Intermediate Thermal Mechanical Treatment on the Fatigue Properties of High Strength Aluminum Alloys, X7091," M.S. Thesis, Georgia Institute of Technology, Atlanta, GA, August, 1981.

References

1. Victor W.C. Kuo and E.A. Starke, Jr., Metall. Trans. A, 1983, vol. 14A, p. 435.

2. J.P. Lyle, Jr. and W.S. Cebulak, Met. Eng. Quart., 1974, vol. 14, no. 1, p. 52.

3. J.P. Lyle, Jr. and W.S. Cebulak, Metall. Trans. A, 1975, vol. 6A, p. 685.

4. W.S. Cebulak, E.W. Johnson, and H. Markus, Met. Eng. Quart., 1976, vol. 16, no. 4, p. 37.

5. S. Hirose and M.E. Fine, High-Strength Powder Metallurgy Aluminum Alloys, M.J. Koczak and G.J. Hildeman, eds., TMS-AIME, Warrendale, PA, 1983, p. 19.

6. M. Rafalin, A. Lawley, and M.J. Koczak, High-Strength Powder Metallurgy Aluminum Alloys, M.J. Koczak and G.J. Hildeman, eds., TMS-AIME, Warrendale, PA, 1983, p. 63.

7. S. L. Langenbeck, High-Strength Powder Metallurgy Aluminum Alloys, M.J. Koczak and G.J. Hildeman, eds., TMS-AIME, Warrendale, PA, 1983, p. 87.

8. Y.W. Kim and L.R. Bidwell, High-Strength Powder Metallurgy Aluminum Alloys, M.J. Koczak and G.J. Hildeman, eds., TMS-AIME, Warrendale, PA, 1983, p. 107.

9. J.R. Pickens, J.R. Gordon, and L. Christodoulou, High-Strength Powder Metallurgy Aluminum Alloys, M.J. Koczak and G.J. Hildeman, eds., TMS-AIME, Warrendale, PA, 1983, p. 177.

10. I.G. Palmer, R.E. Lewis, and D.D. Crooks, Aluminum-Lithium Alloys, T.H. Sanders and E.A. Starke, Jr., eds., TMS-AIME, Warrendale, PA, 1981, p. 241.

11. F.J. Humphreys, Acta Metall., 1977, vol. 25, p. 1323.

12. R.E. Sanders, Jr. and E.A. Starke, Jr., Thermomechanical Processing of Aluminum Alloys, J.G. Morris, ed., TMS-AIME, Warrendale, PA, 1978, p. 50.

13. R.E. Sanders, Jr. and E.A. Starke, Jr., Metall. Trans. A, 1978, vol. 9A, p. 50.

14. J. Lindigkeit, G. Terlinde, A. Gysler, and G. LUtjering, Acta Metall., 1979, vol. 27, p. 1717.

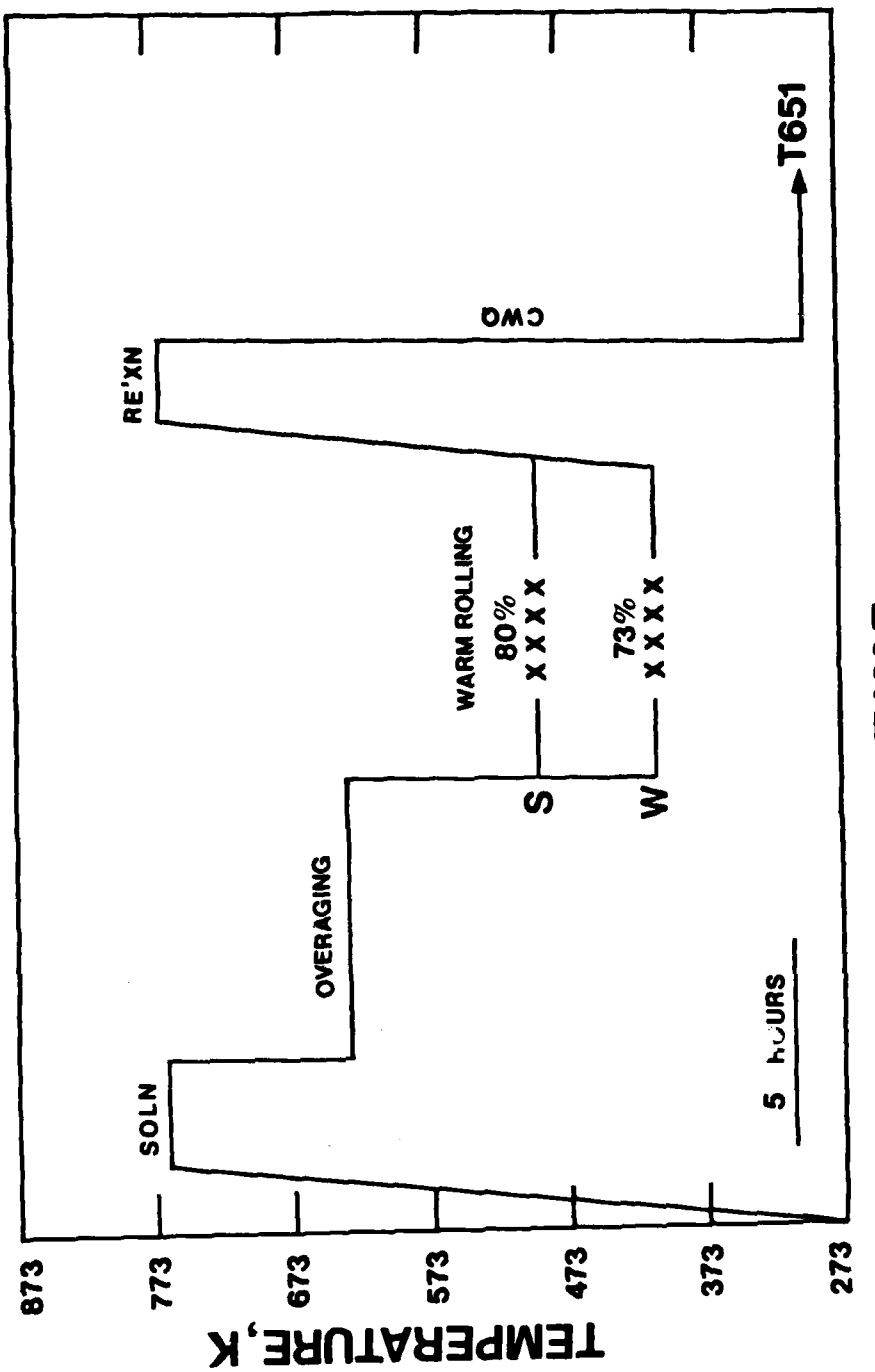

Figure 1. The ITMT schedules used to produce the S and W plates.

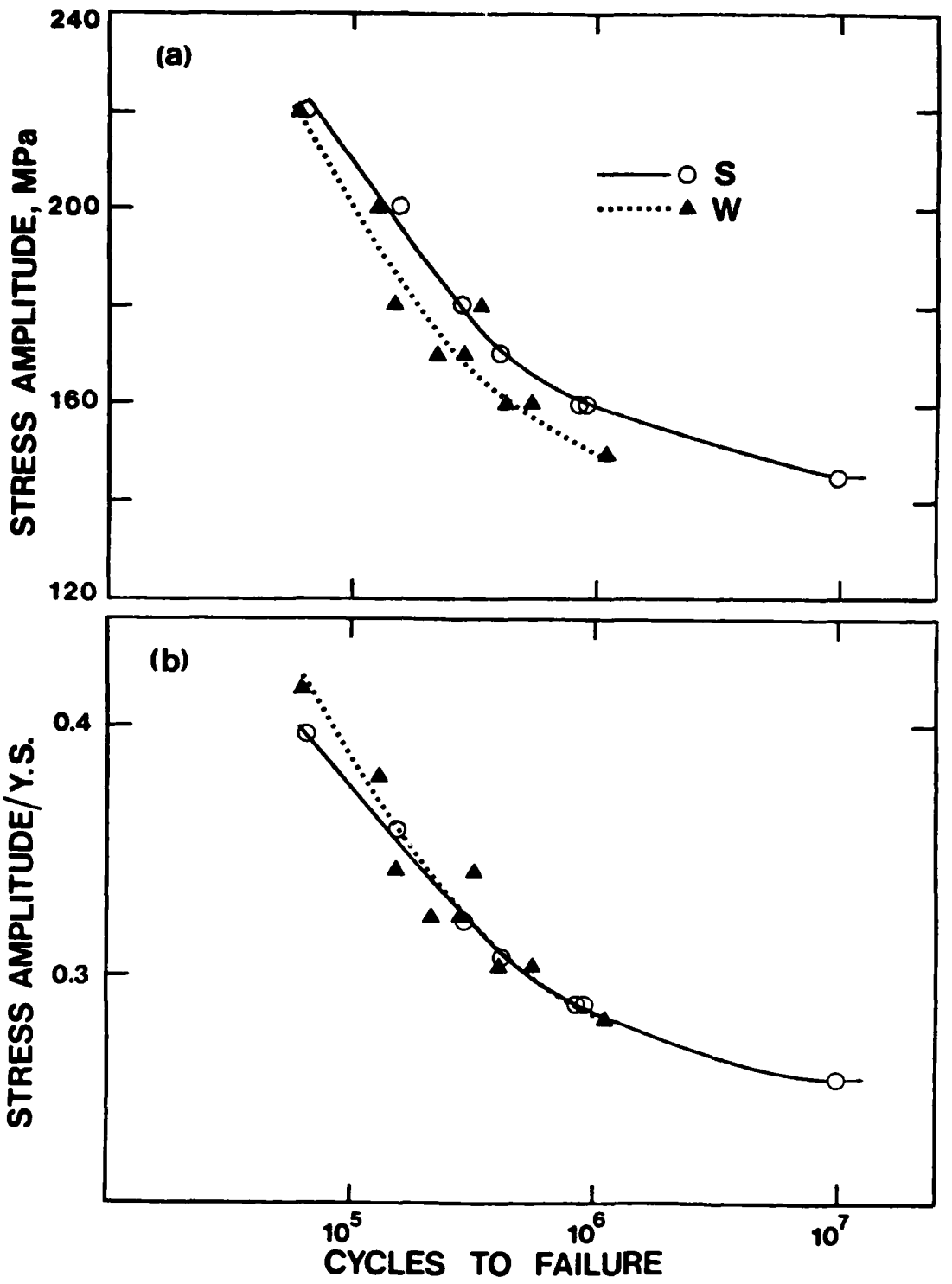

Figure 2. The HCF S-N curves showing (a) stress lives, and (b) normalized stress lives of the S and W plates.

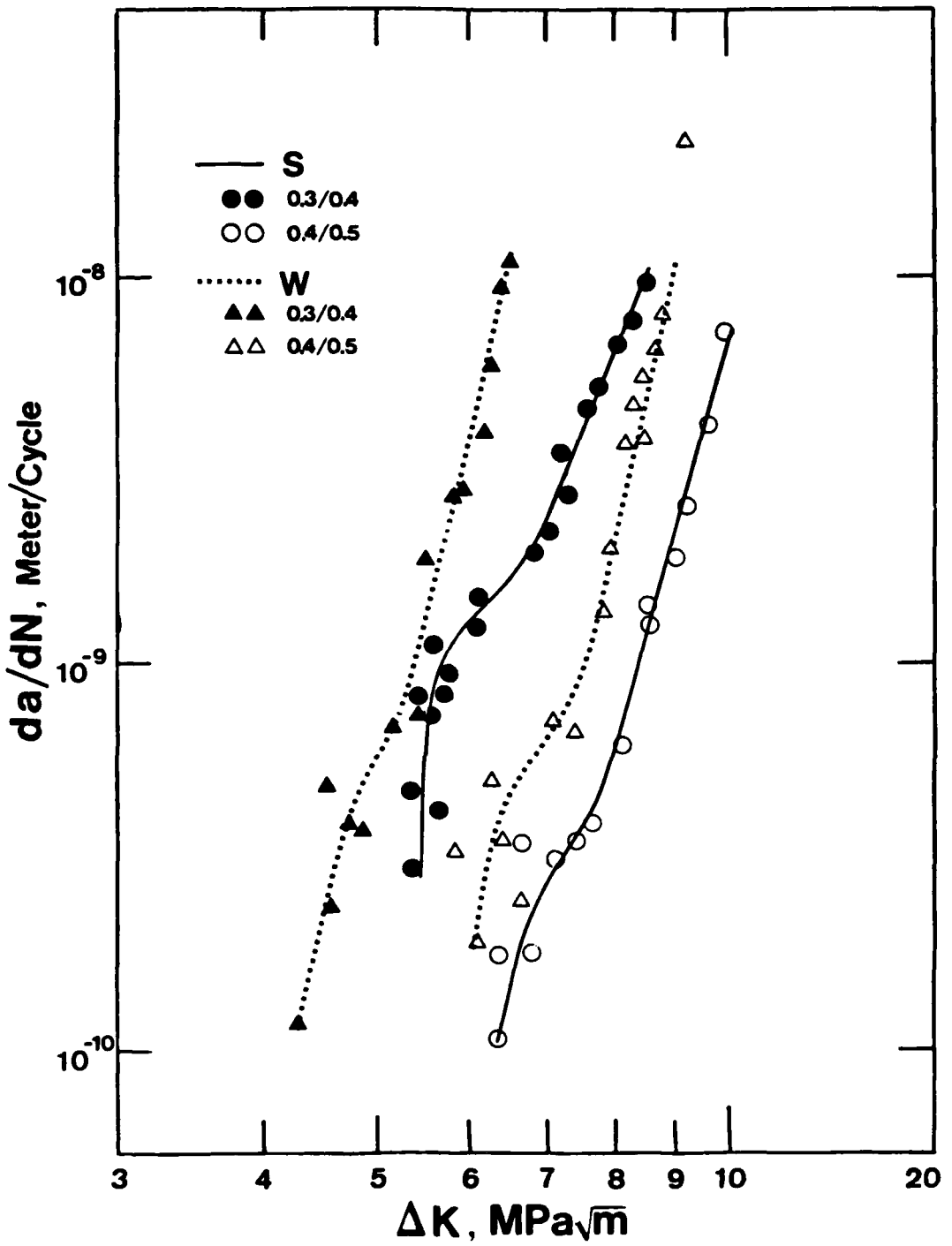

Figure 3. The FCGR's as a function of ΔK for a/w values of 0.3-0.4 and 0.4-0.5, for the S and W plates.

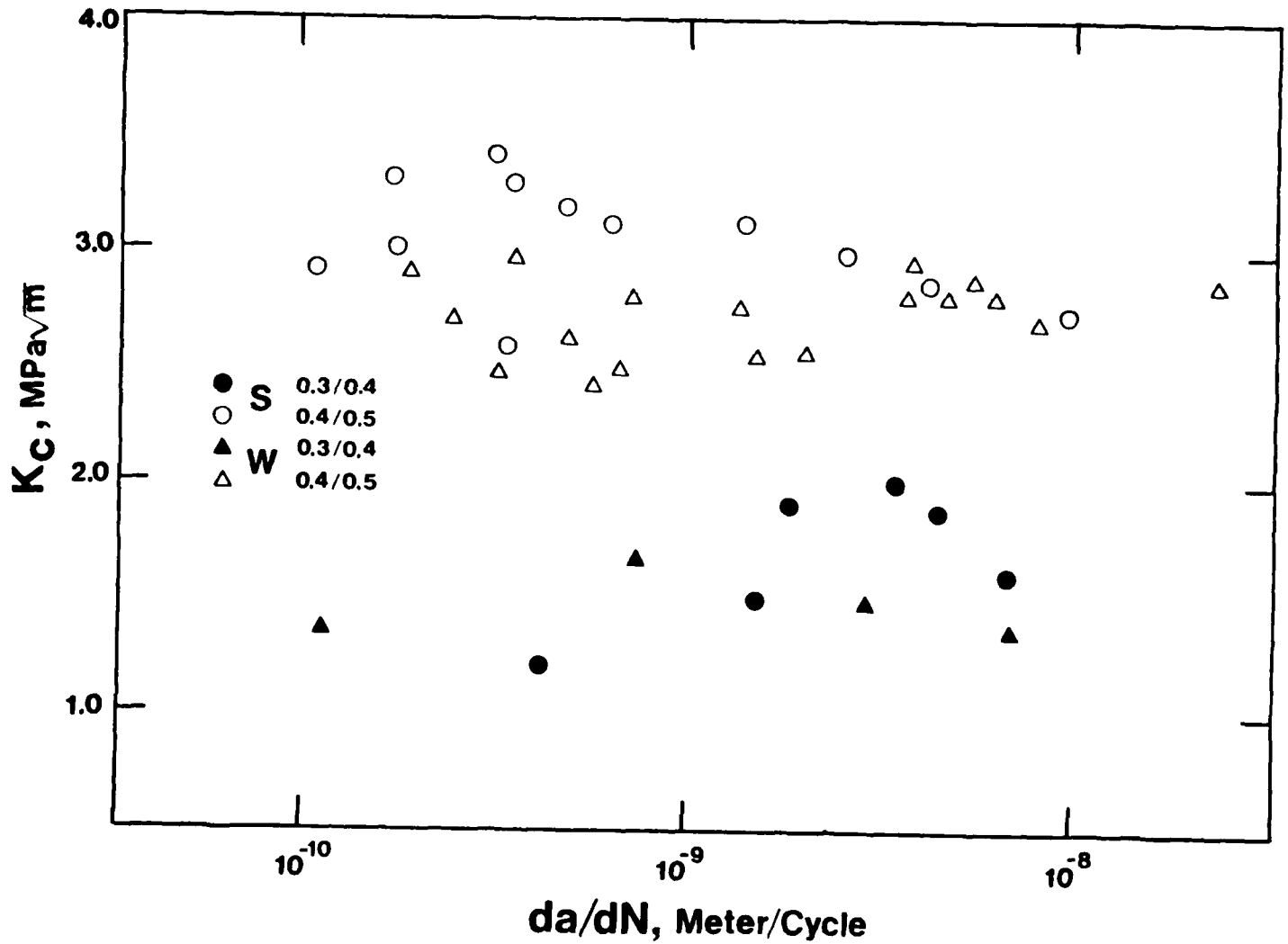

Figure 4. The crack closure stress intensities, K_c's, as a function of FCGR and a/w values for the S and W plates.

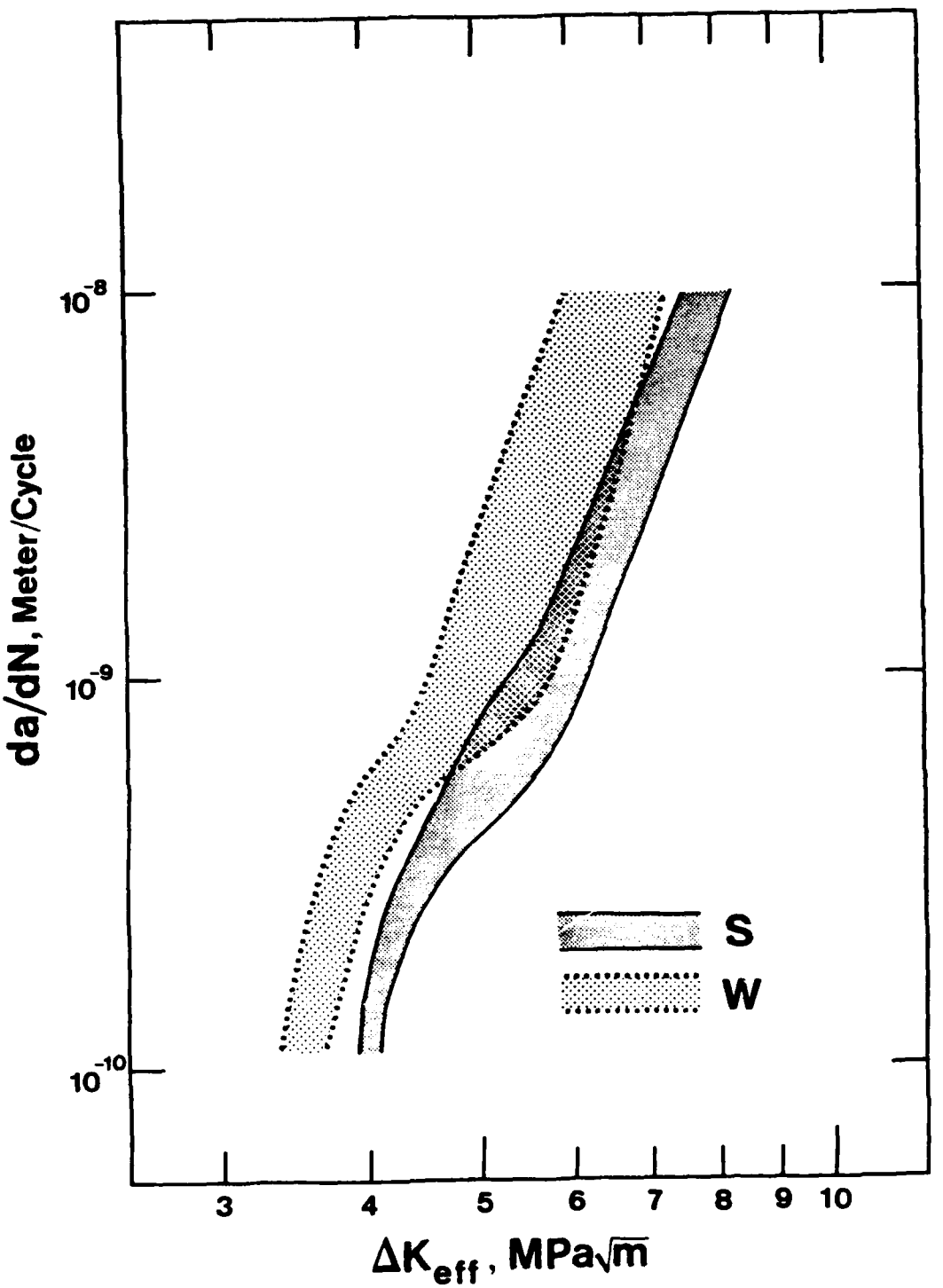

Figure 5. The FCGR's as a function of effective stress intensity, K_{eff}, for the S and W plates.

END

DATE
FILMED

9 — 83

DTIC